

I4 What Aligns Liquid Crystals on Solid Substrates? The Role of Surface Roughness Anisotropy

Satyendra Kumar,^{1,*} Jae-Hoon Kim,^{1,2} and Yushan Shi¹

¹Department of Physics, Kent State University, Kent, Ohio 44240, USA

²Division of Electrical and Computer Engineering, Hanyang University,

Seoul 133-791, Republic of Korea

jhoon@hanyang.ac.kr

The mechanism responsible for liquid crystal (LC) alignment on mechanically buffed or UV exposed polymer films is poorly understood. A comprehensive study of LC alignment on variously prepared substrates unequivocally shows that the anisotropy in the surface roughness of the substrate completely determines the direction of LC alignment. In all the cases studied, including those where an anchoring transition occurs with temperature, the LC director (re)aligns in the directions of low roughness.

1. Introduction

It has been known for a long time that rubbed [1] polymer films, Langmuir-Blodgett (LB) films [2], vacuum deposited dielectric layers [3], polymer films [4] exposed linearly polarized ultraviolet (LPUV) light, photoaligned liquid crystal (LC) [5], and other methods which produce a grooved surface [6] induce alignment of LCs. Berreman [7] suggested that long-range anisotropic elastic effects induced by grooved surfaces are responsible for LC alignment. It was later reported that the surface structures produced upon rubbing a polymer layer may not be responsible for LC alignment [8]. However, these interpretations were based on measurements of surface morphology on a macroscopic (~ μm) length scale and did not address the influence of morphology at a more appropriate microscopic scale. We show here that substrate morphology at sub- μm scales is of great importance in determining LC alignment.

The LC alignment is believed to be influenced by (i) the chemical [8,9] interactions between the alignment layer [10] and the LC, and (ii) the interplay between LC anisotropic elastic properties and the substrate's topography [7]. The specific role that each of these factors plays has been difficult to separate [11] and quantify. The results of our comprehensive high-resolution x-ray

reflectivity [12] (HRXR) and atomic force microscopy (AFM) study [using Nanoscope III (Digital Instruments) in the contact mode] of a large number of alignment layers prepared by different processes establish that the anisotropy in the root mean square (rms) vertical roughness of the substrate's surface fully determines the direction of LC alignment. Chemical interactions between the alignment layer and LC, on the other hand, are expected to determine the polar and azimuthal anchoring energies.

2. Experiment

In this study, we used films or surfaces of commercially available polyvinyl alcohol (PVA), bare glass, linearly photopolymerizable polymer (LPP) [13], polyimide (PI) (SE610, Nissan Chemical Co.), and polystyrene (PS). Different polymers are spin coated and thermally cured per standard prescriptions. Rubbed PI and PS films are selected because they align LCs parallel and perpendicular to the rubbing direction, respectively. The PI, PVA, and PS layers are rubbed by a velvet cloth, bare glass with a scotchguard pad (3M), and LPP films are exposed to LPUV. They can be divided in to two groups: (i) the PI, PVA, and bare glass align LCs parallel to the rubbing direction, and (ii) the LPP and PS films align LCs

perpendicular to the UV's polarization and the rubbing direction, respectively. Additionally, we studied a system [14] [PVA alignment layer reacted with trifluoroacetic anhydride (TFAA) in the gas phase to substitute the polar -OH group by -OCOCF₃] in which the direction of alignment changes with temperature.

The determination of the anisotropy in a film's morphology by HRXR is made possible by inherent unequal x-ray coherence lengths of $\sim 5000\text{\AA}$ and $\sim 60\text{\AA}$ in directions longitudinal and transverse to the direction of incidence, respectively. Specular reflectivity scans are conducted in two different orientations of the sample obtained by 90° rotations about the scattering vector, q (see the inset in Fig. 1) which is perpendicular to the substrate. The x direction is defined to be the direction of treatment (rubbing or the direction of UV's polarization), and the y direction is orthogonal to it. If the surface is anisotropically rough, then the reflectivities measured with x and y directions in the scattering plane are different. Off-specular scans, conducted at an offset of 0.02° from the specular condition, are subtracted from the specular scans and the resultant reflectivity analyzed to obtain σ . The difference, $\Delta\sigma$, between the σ 's obtained for the x and y directions provides a quantitative measure of the surface roughness anisotropy.

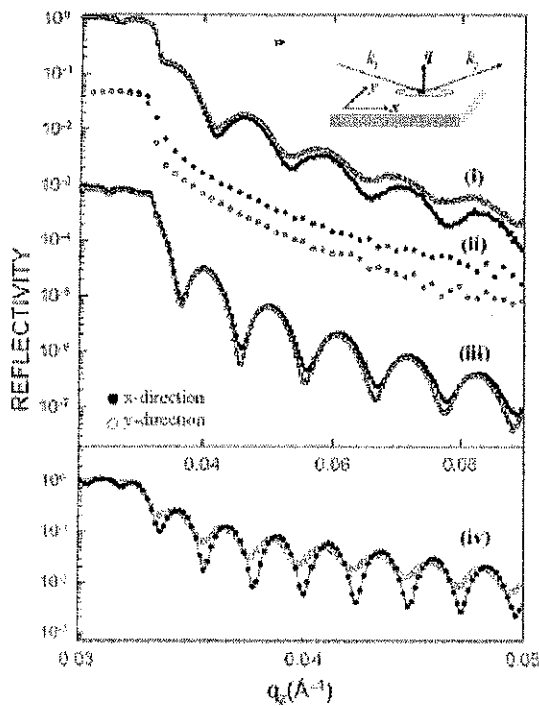


Fig. 1 X-ray reflectivity profiles for x (●) and y (○) directions, in the scattering plane (inset), for (i) $\sim 350\text{\AA}$

rubbed PVA, (ii) rubbed glass, (iii) $\sim 410\text{\AA}$ LPUV exposed LPP, and (iv) 2600\AA rubbed PI films. Curves (ii) and (iii) are shifted down by 1.5 decades each. The horizontal scale for (iv) has been expanded for clarity.

Prior to the treatment, reflectivity scans in the x and y orientations for PI, PVA, bare glass, and LPP are identical, showing that they are initially isotropic. HRXR profiles for the two orientations of rubbed PI, PVA, bare glass, and LPUV exposed LPP films are shown in Fig. 1. Kiessig fringes are clearly seen for all except bare glass. After the treatment, fringes remain brighter in the x direction for rubbed PVA and PI, but in the y direction for LPP. For bare glass, the reflectivity in the y direction diminishes at a faster rate than in the x direction because of the increased roughness anisotropy.

The mechanism which gives rise to the changes in the roughness is, of course, different for each film and depends on the treatment method: the polymer chains in PI and PVA may undergo reorientation upon rubbing [8,10], LPUV exposure causes photopolymerization in LPP film [13], and rubbing should cause simple linear scratches [5] on bare glass. Whatever the mechanisms may be, different treatments induce roughness anisotropy on

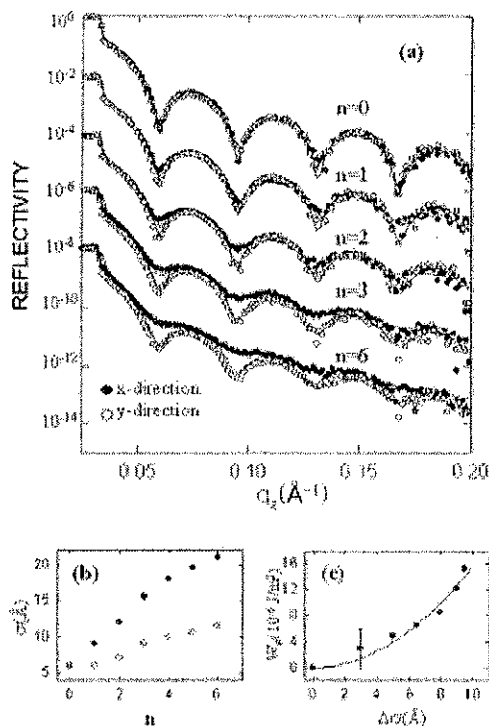


Fig. 2 (a) HRXR profiles for x (●) and y (○) orientations of a $\sim 150\text{\AA}$ thick rubbed PS film with an increasing number, n , of rubbing, the solid lines represent fits. (b) Root mean square roughness σ as a function of

n for the two orientations of the substrate. (c) Dependence of anchoring energy W on the roughness anisotropy $\Delta \sigma$.

substrates' surface. Alignment of LC along the direction of lower roughness, as expected from Berreman's calculation, is found to be a *universal feature of all alignment films* irrespective of how they are prepared.

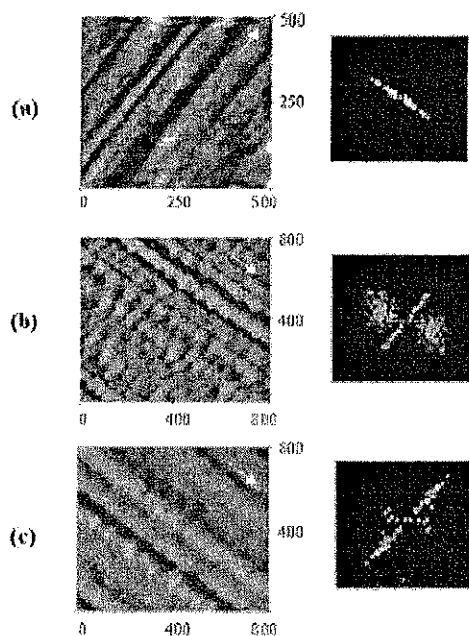
Contrary to the intuitive expectation that a rubbed polymer film should always align LC parallel to the rubbing direction, PS films align [8] LCs perpendicular to the rubbing direction. Figure 2(a) shows the dependence of x-ray reflectivity for such a film on the number of times, n , the film is rubbed. Initially, reflectivities in the x and y orientations yield essentially the same roughness of $\sim 7 \pm 1 \text{ \AA}$. Upon rubbing, the amplitude of Kiessig fringes begins to diminish dramatically in the x direction and remains relatively large in the y direction. The difference grows with n . Results show that the roughness is dramatically increased in the x direction. For $n=6$, the roughness increases to $21 \pm 1 \text{ \AA}$ in the x and $11.5 \pm 1 \text{ \AA}$ in the y direction. The LC aligns along the smoother y direction, i.e., perpendicularly to rubbing.

To further verify this surprising relationship between LC alignment and the surface roughness anisotropy, real space morphologies of rubbed PI and PS surfaces are acquired with the AFM in air at room temperature using a pyramidal shaped Si_3N_4

Fig. 3 AFM images (left) with axes marked in nm's and their power spectra (right) of (a) rubbed PI, (b) rubbed PS, and (c) rubbed PS after annealing. The white arrows mark the rubbing direction.

tip integrated into a rectangular cantilever with a spring constant of 0.58 N/m. The surface morphologies of rubbed PI and PS and their power spectra (Fourier transforms) are shown in Figs. 3(a) and 3(b), respectively. For PI, microscratches and elongated PI structures extending along the rubbing direction are clearly visible. The morphological anisotropy, revealed in a highly directional power spectrum, is induced purely by the physical modification of the surface during mechanical rubbing.

The rubbed PS film presents a very puzzling yet fascinating case. In addition to the scratch lines, Fig. 3(b), there are elongated polymer structures in the orthogonal direction which develop during rubbing. The power spectrum also shows an additional component (not seen for PI) in the direction approximately perpendicular to the linear component corresponding to the scratches. This new component resembles powder x-ray diffraction peaks and suggests a weakly periodic nature of these polymer structures. These polymer structures render the direction orthogonal to the rubbing direction statistically smoother along which the LC aligns. Figure 3(c) shows the surface morphology of the rubbed PS film after thermal annealing at 100°C for 30 min. The scratch lines as well as the orthogonal polymer structures become obscure. Consequently, both branches in the power spectrum also diminish upon annealing. A homogeneously



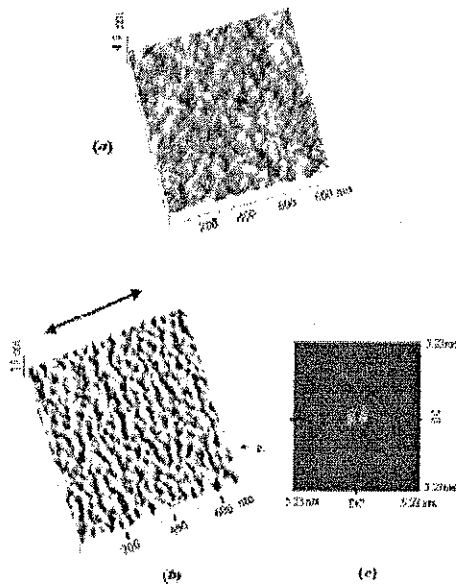


Fig. 4 AFM images of a $\sim 110\text{\AA}$ thick PVMC film (a) before and (b) after LPUV exposure. The arrow in (b) indicates the direction of UV's polarization, and (c) the power spectrum of (b).

aligned LC cell, prepared with twice rubbed PS substrates, loses alignment and develops schlieren texture upon annealing. Clearly, morphological changes are directly responsible for the alignment and, subsequently, its loss upon annealing. It can be concluded that the anisotropy in the surface morphology in general, and over the length scale of the x-ray beam's coherence length ($\sim 5000\text{\AA}$) in particular, determines the direction of alignment. No exceptions to this rule are found in more than 30 alignment layers of different types studied by us which include LB film [12], liquid crystalline polymer film aligned on LPP film, and LPUV exposed poly(vinyl 4-methoxy-cinnamate) [12] (PVMC). In the case of PVMC, random surface structures of a fresh film, Fig. 4(a), change to anisotropic ridgelike structures, Fig. 4(b), oriented perpendicularly to the polarization of LPUV. The power spectrum, Fig. 4(c), of the AFM image taken after LPUV treatment clearly confirms the existence of morphological anisotropy.

3. Result and Discussion

To ascertain the role of chemical interactions, we measure azimuthal anchoring energy, W , for rubbed PS films and quantitatively examine its dependence on the surface roughness anisotropy. The energy W should encompass the effects of chemical interaction between the LC and the alignment layer

as well as the morphological effects. A mixture of the nematic LC 5CB (British Drug House) and chiral dopant (S811) is injected into a wedge cell prepared with rubbed PS substrates and the director inclination angle at the surface is measured under a polarizing microscope and the value of W calculated [15]. W is found to increase [Fig. 2(c)] with the roughness anisotropy, $\Delta\sigma$, which in turn depends on the number of rubbings, as shown in Fig. 2(b). It should be noted that the macroscopic roughness of a surface is known to scale with its microscopic roughness. Now, according to Berreman [7], surface anchoring energy should increase quadratically with the surface undulation height, or the roughness anisotropy. The solid line fit in Fig. 2(c) represents a quadratic dependence of the anchoring energy on the roughness anisotropy. The proportionality constant required to fit the data is expected to depend on the nature and the strength of chemical interactions between the alignment layer and the liquid crystal.

The relationship between the LC alignment and

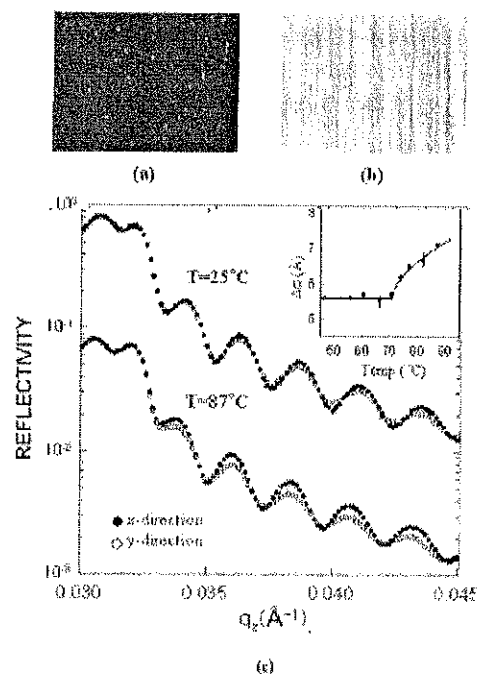


Fig. 5 Optical micrographs of (a) homeotropic TFAA cell, at 25°C , which undergoes an anchoring transition to (b) homogeneous alignment at 87°C . The white specs in (a) are defects. (c) Reflectivities indicate increasing roughness anisotropy (inset) with temperature above 75°C for a $\sim 2500\text{\AA}$ thick TFAA film.

surface roughness anisotropy is further tested on TFAA films that exhibit an anchoring transition with temperature resulting in a change from

homeotropic to planar (i.e., random in plane) or to homogeneous (on films which were rubbed prior to fluorination) LC orientation. Figures 5(a) and 5(b) show the LC (E48) textures in a cell made with TFAA films at 25 and 87°C, respectively. Such films exhibit the anchoring transition at ~75°C. Measured reflectivities, Fig. 5(c), reveal an increasing difference in the Kiessig fringes' amplitude above this temperature. The anisotropy $\Delta\sigma$ is small and temperature independent below 75°C; see the inset in Fig. 5. It begins to increase above this temperature and the alignment changes to homogeneous. This provides further evidence that alignment is primarily driven by the surface roughness anisotropy.

4. Conclusion

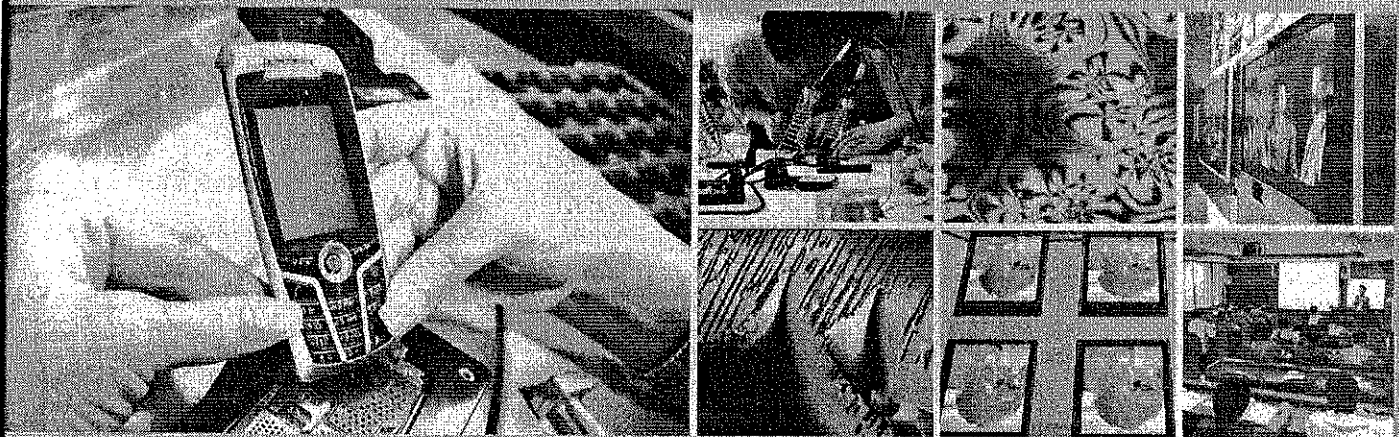
In conclusion, the anisotropy in surface morphology of a substrate on a submicron length scale appears to play the defining role in determining the direction of LC alignment and the increase in anchoring energy with $\Delta\sigma$ (or degree of rubbing). However, overall strength of the anchoring energy is expected to primarily depend on chemical interactions between the LC and the alignment layer. This is analogous to the necessary (but not sufficient) requirement that the shape of molecules be anisotropic for the formation of a LC phase. Just as the physical properties of a LC such as viscosity, birefringence, transitions temperatures, and transition enthalpies depend on intermolecular interactions, the anchoring energy of a LC depends on the interfacial roughness anisotropy and interactions between the LC and the interface.

Acknowledgement

This work was supported, in part, by NSF Grants No. DMR-89-20147 and No. DMR-03-12792 and by Korea Research Foundation Grant No. KRF-2004-005-D00165. The authors thank Dr. Martin Schadt for very helpful discussions and for supplying the LPP samples.

References

- [1] C. Mauguin, Bull. Soc. Fr. Mineral. **34**, 71 (1911); J. Cognard, Mol. Cryst. Liq. Cryst., Suppl. Ser. 1, 1 (1982).
- [2] T. Seki et al., Macromolecules **22**, 3505 (1989).
- [3] J. L. Janning, Appl. Phys. Lett. **21**, 173 (1972).
- [4] M. Schadt, H. Seiberle, and A. Schuster, Nature (London) **381**, 212 (1996); J.-H. Kim, Y. Shi, S.-D. Lee, and S. Kumar, Phys. Rev. E **57**, 5644 (1998).
- [5] Y. Reznikov et al., Phys. Rev. Lett. **84**, 1930 (2000).
- [6] D. C. Flanders, D. C. Shaver, and H. I. Smith, ppl. Phys. Lett. **32**, 597 (1978); R. R. Shah and N. L. Abbott, Science **293**, 1296 (2001); J.-H. Kim, M. Yoneya, H. Yokoyama, Nature (London) **420**, 159 (2002).
- [7] D.W. Berreman, Phys. Rev. Lett. **28**, 1683 (1972); Mol. Cryst. Liq. Cryst. **23**, 215 (1973); P. Patri'cio et al., Phys. Rev. Lett. **88**, 245502 (2002).
- [8] J. M. Geary, J.W. Goodby, A.R. Kmetz, and J. S. Patel, J. Appl. Phys. **62**, 4100 (1987); D.-S. Seo et al., Mol. Cryst. Liq. Cryst. **231**, 95 (1993).
- [9] J. Stohr et al., Macromolecules **31**, 1942 (1998).
- [10] M. F. Toney et al., Nature (London) **374**, 709 (1995).
- [11] W. Chen, M. B. Feller, and Y. R. Shen, Phys. Rev. Lett. **63**, 2665 (1989).
- [12] B. Cull, Y. Shi, M. Schadt, and S. Kumar, Phys. Rev. E **53**, 3777 (1996); B. E. Warren, X-ray Diffraction (Dover, New York, 1969).
- [13] M. Schadt, K. Schmitt, V. Kozinkov, and V. Chigrinov, Jpn. J. Appl. Phys. **31**, 2155 (1992).
- [14] K. Ha and J. L. West, Liq. Cryst. **31**, 753 (2004).
- [15] Y. Sato, K. Sato, and T. Uchida, Jpn. J. Appl. Phys. **31**, L579 (1992).



Proceeding of 8th
**KOREAN LIQUID CRYSTAL
CONFERENCE**

2005. 8. 19 (Friday) ~ 20(Saturday)

Organized by

KIΔΣ  Korea Liquid Crystal Society

 Display Technology Education Center at Hoseo University

CONTENTS

INVITED and ORALS

- I-1. Liquid Crystalline Order for Organic Electronics and Biotechnologies** **1**
Sin-Doo Lee, Seoul National University
- I-2. Alignment technologies of liquid crystals: Status of rubbing, photo-, and ion-beam alignment** **33**
Masaki Hasegawa, IBM Tokyo Research Lab.
- I-3. Advanced Liquid Crystal Materials for TFT Applications** **37**
Min Ok Jin, Merck Korea Co.
- I-4. What is really responsible for the LC alignment on substrate?** **61**
Jae Hoon Kim, Hanyang University
- O1. Synthesis and mesomorphic properties of new chiral bent-core mesogens with chiral (alkyloxy)alkoxy terminal groups** **66**
K.-T. Kang¹, S.K. Lee¹, S.Heo¹, J.G.Lee¹, K.Kumazawa², K.Nishida², Y.Shimbo², Y.Takanishi², J.Watanabe², and H.Takezoe²
¹Pusan National University, ²Tokyo Institute of Technology.
- O2. Novel Liquid Crystal Alignment Method: Ion Beam technique and its applications** **72**
Han Jin Ahn, Kyung Chan Kim, Jong Bok Kim, Byoung Har Hwang, and Hong Koo Baik, Yonsei University
- O3. Surface Interaction Effects on Anisotropic Phase Separation of Polymer and Liquid Crystal Composite System** **76**
Min Young Jin, Tae-Hee Lee, Jong-Wook Jung, and Jae-Hoon Kim, Hanyang University
- O4. A Single Step Patterning of the Retardation Layer for a Transflective LCD with a Single LC Mode** **80**
Yong-Woon Lim, Jinyool Kim, and Sin-Doo Lee, Seoul National University
- O5. Observation of Textures due to Carbon Nanotubes Dispersion in an In-Plane Switching Liquid Crystal Cell** **85**
J.-H. Choi¹, I.-S. Baik¹, K. H. An², S. H. Lee¹, and Y. H. Lee²
¹Chonbuk National University, ²Sungkyunkwan University